Anomalous penetrant transport in glassy polymers: 4. Stresses in partially swollen polymers

John Klier and Nikolaos A. Peppas
School of Chemical Engineering, Purdue University, West Lafayette, IN 47907, USA
(Received 17 July 1986; revised 16 January 1987; accepted 31 March 1987)

The equilibrium swelling process and stress evolution of glassy polymer systems undergoing Case-II penetrant transport were examined using a rubber elasticity theory. Consideration of coupling between stresses and penetrant concentration permitted calculation of equilibrium stress and concentration profiles for a variety of molecular and geometric factors.

(Keywords: Case-II transport; penetrant transport; anomalous transport; rubber elasticity; glassy polymers; stresses in polymers)

INTRODUCTION

Investigation of the transport behaviour of penetrants in glassy polymers frequently reveals mass uptake of penetrant which does not obey Fick's law[1]. Initial weight gain can be proportional to t^n, where t is time and n is an exponent greater than 0.5, rather than $t^{0.5}$ as predicted by the solution to Fick's law. This anomalous transport has been the subject of a number of theoretical and experimental analyses.

Frisch *et al.*[2] first proposed a modified Fick's law flux equation by superimposing a stress-induced velocity term with a Fick's law type concentration gradient-driven flux. A phenomenological approach was used by Peterlin[3,4] to describe transport behaviour in systems which exhibit anomalous transport behaviour with a constant velocity moving front which separates the swollen rubbery from the unswollen glassy polymer. This approach was used to calculate concentration profiles for diffusion in the glassy region of the polymer preceding the moving front.

In order to explain two-stage sorption behaviour, Astarita and his collaborators[5,6] considered the coupling of relaxational surface and diffusive behaviour in swollen polymer films. They developed a mathematical model for penetrant uptake based on an empirical constitutive model. Their analysis gave good agreement with experimental results.

The effects of simultaneous bulk relaxational and diffusive phenomena were treated by Thomas and Windle[7]. Consideration of the penetrant-induced osmotic stresses resulted in a time-dependent component of penetrant mass uptake, and, thus in anomalous behaviour. Durning[8] modelled anomalous penetrant transport by using a constitutive equation which expresses penetrant flux as a function of concentration and stress gradient contributions. According to this model, relaxation of penetrant-induced stresses gives rise to anomalous uptake behaviour. Other theoretical and experimental developments concerning the mechanism of anomalous transport are summarized in a recent review by Windle[1].

The preceding models focus on the mechanisms of anomalous penetrant transport. This paper concentrates, instead, on determination of the penetrant concentration and stress profiles in the swollen rubbery portion of a polymer which undergoes Case-II transport. Certain physical characteristics of Case-II transport are incorporated in the analysis presented below. The underlying mechanism of Case-II transport, however, is not addressed explicitly.

Case-II transport is a specific type of anomalous transport, first defined by Alfrey *et al.*[9]. The polymer undergoing this penetrant transport exhibits a sharp front which separates the glassy from the rubbery regions and which moves at a constant rate with respect to the observer's frame of reference. The penetrant in the rubbery region is at equilibrium with the surrounding penetrant, whereas the glassy region contains a very small amount of penetrant. The distribution of stresses in polymer discs and cylinders undergoing Case-II transport was first examined by Alfrey *et al.*[9]. They used a linear elastic model for small strains to solve for stresses, and neglected the coupling between stress and swelling.

The analysis presented below treats the case of a polymer with an unswollen, rigid, glassy core adjacent to a swollen, rubbery region which is at equilibrium with the surrounding penetrant. By applying the theory of rubber elasticity to the swollen portion of the polymer and taking advantage of relationships between stress and swelling for systems at equilibrium, it is possible to predict stress and concentration evolution in systems of varying geometry. This analysis may be applied to Case-II transport or anomalous transport which exhibit equilibrium between the steady state of the penetrant in the swollen region and the surrounding penetrant, as well as to any other problems which have analogous swelling characteristics and geometric constraints.

THEORETICAL TREATMENT

General

Consider the deformation of a rubbery polymer along

0032-3861/87/111851-09$03.00

three axes, where λ_i is the extension ratio along the ith principal axis. The extension ratio is the ratio of the length of the deformed sample along the axis of deformation to that of the undeformed sample.

Valanis and Landel[10] have shown that the work $W(\lambda_1, \lambda_2, \lambda_3)$ involved in a deformation can be written as a sum of components, $w(\lambda_i)$, i.e., the components of this work function specific to the principal extension ratios, λ_i. The corresponding differences in stress along the axes i and j are

$$\sigma_i - \sigma_j = \lambda_i w'(\lambda_i) - \lambda_j w'(\lambda_j) \quad (1)$$

or equivalently

$$\sigma_i = \lambda_i w'(\lambda_i) + p \quad (2)$$

Here σ_i is the force per unit area of the deformed sample along the ith principal deformation axis, $w'(\lambda_i)$ is the derivative of $w(\lambda_i)$ with respect to λ_i, and p is an arbitrary isotropic force which can be a hydrostatic pressure.

For a swollen material we can write[11]

$$\sigma_i = \lambda_i v_2 w'(\lambda_i) + p \quad (3)$$

where now λ_i are the extension ratios with respect to the unswollen, unstrained material and v_2 is the equilibrium polymer volume fraction in the gel.

From the kinetic analysis of Flory and Erman[12-15]

$$w(\lambda_i) = \left(\frac{\xi kT}{2V_0}\right)\left\{\lambda_i^2 - 1 + \frac{\mu}{\xi}[(1+g_i)B_i - \ln[(B_i+1)(g_iB_i+1)]]\right\} \quad (4)$$

with B_i and g_i defined as

$$B_i = \frac{(\lambda_i - 1)(1 + \lambda_i - \zeta\lambda_i^2)}{(1+g_i)^2} \quad (5)$$

$$g_i = \lambda_i^2[\kappa^{-1} + \zeta(\lambda_i - 1)] \quad (6)$$

$$G = \frac{\xi kT}{V_0} \quad (7)$$

Here, κ and ζ are parameters characterizing the degree of polymer entanglement and entanglement response to deformation, respectively. The parameter κ represents the constraint on the junction fluctuations by network entanglements and ζ gives the response of the domains of constraint to network distortions in the Flory–Erman theory[13,15]. The elastic modulus, G, is expressed by equation (7), where ξ is the cycle rank of the network, μ/ξ is a measure of the functionality of the network (equal to one for a perfect tetrafunctional network), and V_0 is the volume of the unswollen, unstrained network. The cycle rank of the network, ξ, is a measure of the number of complete loops formed by crosslinked polymer chains, and is therefore a measure of the degree of crosslinking of the network.

The term $(\lambda_i^2 - 1)$ of equation (4) is the strain energy term corresponding to the phantom network model, whereas the remainder is the term arising from constraints on junction fluctuations by surrounding chains.

Erman[15] has shown that the first term of the right-hand side of equation (3) can be written using equation (4) as

$$\lambda_i v_2 w'(\lambda_i) = \lambda_i^2 v_2 G\left[1 + \frac{\mu}{\xi} K(\lambda_i^2)\right] \quad (8)$$

where

$$K(\lambda_i^2) = B(B'(B+1)^{-1} + g(g'B + gB')(gB+1)^{-1}) \quad (9)$$

$$B' = \frac{\partial B}{\partial \lambda_i^2} \quad (10)$$

and

$$g' = \frac{\partial g}{\partial \lambda_i^2} \quad (11)$$

Thus, using the Flory–Erman theory of network elasticity, equation (3) can be written as

$$\sigma_i = \lambda_i^2 v_2 G\left[1 + \frac{\mu}{\xi} K(\lambda_i^2)\right] + p \quad (12)$$

Consequently, the stress differences become

$$\sigma_i - \sigma_j = v_2 G\left[\lambda_i^2 - \lambda_j^2 + \lambda_i^2 \frac{\mu}{\xi} K(\lambda_i^2) - \lambda_j^2 \frac{\mu}{\xi} K(\lambda_j^2)\right] \quad (13)$$

This result holds for any state of strain or swelling.

Calculation of stresses in partially swollen slabs, spheres and cylinders

The computation of stresses in swelling slabs, spheres and cylinders can be accomplished by specifying conditions of mechanical equilibrium, appropriate boundary conditions and a constitutive equation for stress–strain relationships. The conditions for mechanical equilibrium are specific to each geometry and are given in the following derivation. The boundary condition used is that of negligible external force and, consequently, the normal stress at the polymer/penetrant interface is taken to be zero. This condition neglects the effects of external pressure. Body forces are also neglected.

For penetrant transport in a glassy polymer in the form of a slab in which a glassy core is being replaced by a swollen rubbery region, the glassy core constrains the swelling along the y and z axes. We identify the axes x, y and z by the subscripts 1, 2 and 3, respectively, and recognize that the force on the face perpendicular to the x axis must be zero. From the force balance equation[16]

$$\frac{d\sigma_1}{dx} = 0 \quad (14)$$

with the aforementioned boundary conditions, we obtain

$$\sigma_1 = 0 \quad (15)$$

Thus, from equation (13),

$$\sigma_2 = -v_2 G\left[\lambda_1^2 - \lambda_2^2 + \lambda_1^2 \frac{\mu}{\xi} K(\lambda_1^2) - \lambda_2^2 \frac{\mu}{\xi} K(\lambda_2^2)\right] \quad (16)$$

Since the deformations along the y and z directions are identical we also have

$$\sigma_3 = \sigma_2 \quad (17)$$

The extension ratios, λ_i can be specified from geometric constraints on the slab. Two of these extension ratios are

$$\lambda_2 = \lambda_3 = 1 \quad (18)$$

Since the slab cannot expand in the y or z directions the third extension ratio is

$$\lambda_1 = \frac{1}{v_2} \quad (19)$$

Thus, the stresses for a swelling slab can be readily

specified using equations (16)–(19) for a given value of v_2.

For penetrant transport in a spherical system the subscripts 1, 2 and 3 are identified with the r, θ and ϕ directions, respectively. The force balance condition at mechanical equilibrium with negligible external body forces is

$$\frac{d\sigma_1}{dr}=\frac{2}{r}(\sigma_2-\sigma_1) \tag{20}$$

Using equation (13), equation (20) becomes

$$\frac{d\sigma_1}{dr}=-\frac{2}{r}v_2G\left[\lambda_1^2-\lambda_2^2+\lambda_1^2\frac{\mu}{\xi}K(\lambda_1^2)-\lambda_2^2\frac{\mu}{\xi}K(\lambda_2^2)\right] \tag{21}$$

From the boundary condition, $\sigma_1(r_0)=0$, where r_0 is the outer radius of the rubbery region, the following equation for the radial stress can be obtained:

$$\sigma_1(r)=2G\int_r^{r_0}\frac{v_2}{r}\left[\lambda_1^2-\lambda_2^2+\lambda_1^2\frac{\mu}{\xi}K(\lambda_1^2)-\lambda_2^2\frac{\mu}{\xi}K(\lambda_2^2)\right]dr \tag{22}$$

The solutions for $\sigma_2(r)$ and $\sigma_3(r)$ are readily obtained with the aid of equation (13).

To evaluate the term λ_i, the geometric constraints must be considered. The extension ratios resulting from these constraints are

$$\lambda_1=\frac{dr}{dR}=\frac{1}{v_2}\frac{R^2}{r^2} \tag{23}$$

$$\lambda_2=\frac{r}{R} \tag{24}$$

$$\lambda_3=\lambda_2 \tag{25}$$

where

$$R^3=3\int_0^r v_2(r)r^2\,dr \tag{26}$$

The term r is the radial position of interest of the swollen polymer and R is the corresponding radius of the unswollen sample.

For penetrant transport in an infinite cylinder which is constrained to its unswollen dimension in the z direction the subscripts 1, 2 and 3 correspond to r, θ and z, respectively, and the extension ratios are written as

$$\lambda_1=\frac{dr}{dR}=\frac{1}{v_2}\frac{R}{r} \tag{27}$$

$$\lambda_2=\frac{r}{R} \tag{28}$$

$$\lambda_3=1 \tag{29}$$

where

$$R^2=2\int_0^r v_2(r)r\,dr \tag{30}$$

Using the expression for mechanical equilibrium in a cylinder[16]

$$\frac{d\sigma_1}{dr}=\frac{1}{r}(\sigma_2-\sigma_1) \tag{31}$$

Then, equation (32) is readily obtained, in a manner analogous to the spherical case.

$$\sigma_1=G\int_r^{r_0}\frac{v_2}{r}\left[\lambda_1^2-\lambda_2^2+\lambda_1^2\frac{\mu}{\xi}K(\lambda_1^2)-\lambda_2^2\frac{\mu}{\xi}K(\lambda_2^2)\right]dr \tag{32}$$

The foregoing equations specify the stress in a slab which is constrained to uniaxial swelling, a cylinder which is constrained along the z axis, and a sphere, all of which have glassy cores. The concentration profiles in these three objects can be arbitrarily specified without constraints regarding the thermodynamic equilibrium of the penetrant–polymer system. Only the mechanical equilibrium condition of the swollen polymer need be specified. The next step in this development is the specification of the thermodynamic equilibrium between the penetrant in the polymer and the surrounding bath of penetrant.

Relations between stress and equilibrium swelling

In many cases of penetrant transport, the polymer exhibits a front between an equilibrium-swollen rubbery portion and a rigid, unswollen glassy portion. In order to compute the stress we must compute the equilibrium concentration in the rubbery region of the polymer matrix. However, it is important to recognize that the stress and the equilibrium conditions are coupled, that is, the equilibrium polymer volume fraction $v_{2,eq}$ depends on σ_i and *vice versa*.

From Treloar[11] and Erman[15] the expression for σ_i at equilibrium is

$$\sigma_i=2v_2\lambda_i^2\frac{\partial\Delta A_{el}}{\partial\lambda_i^2}+\frac{1}{\bar{V}_1}\frac{\partial\Delta A_{mix}}{\partial n_1} \tag{33}$$

Here ΔA_{el} is the elastic free energy, ΔA_{mix} is the free energy of mixing, $\bar{V}_1$ is specific volume of penetrant, and n_1 is number of moles of penetrant. The first term on the right-hand side represents the resistance to swelling and stress by elastic forces, and the second term represents the tendency of the material to swell due to polymer solvent interactions.

The free energy of polymer penetrant mixing can be expressed using the Flory–Huggins mean field expression

$$\frac{\partial\Delta A_{mix}}{\partial n_1}=RT(\ln(1-v_2)+v_2+\chi v_2^2) \tag{34}$$

where χ is the Flory polymer–penetrant interaction parameter. Furthermore, by using the Flory–Erman[13] expression for elasticity presented in equation (12), equation (33) becomes

$$\sigma_i=\lambda_i^2v_2G\left[1+\frac{\mu}{\xi}K(\lambda_i^2)\right]+\frac{RT}{\bar{V}_1}[\ln(1-v_2)+v_2+\chi v_2^2] \tag{35}$$

This expression allows one to solve for the equilibrium concentration and stresses in a slab upon substitution of the extension ratio, λ_i, for its equivalent values from equations (18) or (19). Recognizing that, for a slab, $\sigma_1=0$ we obtain

$$\frac{G}{v_2}\left[1+\frac{\mu}{\xi}K(\lambda_1^2)\right]+\frac{RT}{\bar{V}_1}[\ln(1-v_2)+v_2+\chi v_2^2]=0 \tag{36}$$

For a phantom network this equation reduces to

$$\frac{G}{v_2}+\frac{RT}{\bar{V}_1}[\ln(1-v_2)+v_2+\chi v_2^2]=0 \tag{37}$$

Solution of this expression for v_2 and substitution of this value into the expressions for σ_2 and σ_3 as shown in equations (16) and (17) gives values for all stresses in the slab undergoing Case-II transport.

The solutions for concentration and stress profiles in the cylinder and sphere are somewhat more complicated. In a slab the unswollen portion of the slab constrains the rubbery portion in the y and z directions. In the cylinders and spheres, however, the additional requirement that a swollen annulus remain in contact with the glassy core provides additional geometric constraints.

For a cylinder, the condition for mechanical equilibrium is given by equation (31) and the corresponding expressions for σ_1 and $(\sigma_2-\sigma_1)$ are given by equations (35) and (13), respectively. Substitution of equation (35) into equation (31) gives

$$\frac{d\sigma_1}{dr}=G\left(2\lambda_1 v_2\frac{d\lambda_1}{dr}+\lambda_1^2\frac{dv_2}{dr}\right)\left[1+\frac{\mu}{\xi}K(\lambda_1^2)\right]+2G\frac{\mu}{\xi}K'(\lambda_1^2)\lambda_1^3 v_2\frac{d\lambda_1}{dr}+\frac{RT}{\bar{V}_1}\left(2\chi-\frac{1}{1-v_2}\right)v_2\frac{dv_2}{dr} \tag{38}$$

where

$$K'=\frac{\partial K}{\partial\lambda^2} \tag{39}$$

Further calculations reveal that

$$\frac{d\lambda_1}{dr}=-\lambda_1\frac{1}{r}-\frac{\lambda_1}{v_2}\frac{dv_2}{dr}+\frac{1}{\lambda_1 v_2 r} \tag{40}$$

Recalling the relationship of equation (27), the previous analysis gives

$$\frac{d\sigma_1}{dr}=\frac{dv_2}{dr}\left\{\frac{RT}{V_1}\left(2\chi-\frac{1}{1-v_2}\right)v_2-G\lambda_1^2\left[1+\frac{\mu}{\xi}K(\lambda_1^2)+2\lambda_1^2\frac{\mu}{\xi}K'(\lambda_1^2)\right]-\frac{2G}{r}\left\{\lambda_1^2 v_2\left[1+\frac{\mu}{\xi}K(\lambda_1^2)+\lambda_1^2\frac{\mu}{\xi}K'(\lambda_1^2)\right]-\left[1+\frac{\mu}{\xi}K(\lambda_1^2)+\lambda_1^2\frac{\mu}{\xi}K'(\lambda_1^2)\right]\right\}\right\} \tag{41}$$

Finally, by combining equations (13), (31) and (41) it is possible to find an expression for dv_2/dr

$$\frac{dv_2}{dr}=\frac{G}{r}\left\{v_2\left[\lambda_2^2-\lambda_1^2+\lambda_2^2\frac{\mu}{\xi}K(\lambda_2^2)-\lambda_1^2\frac{\mu}{\xi}K(\lambda_1^2)\right]+2\lambda_1^2 v_2\left[1+\frac{\mu}{\xi}K(\lambda_1^2)+\lambda_1^2\frac{\mu}{\xi}K'(\lambda_1^2)\right]-2\left[1+\frac{\mu}{\xi}K(\lambda_1^2)+\lambda_1^2\frac{\mu}{\xi}K'(\lambda_1^2)\right]\right\}\times\left\{\frac{RT}{V_1}\left(2\chi-\frac{1}{1-v_2}\right)v_2-G\lambda_1^2\left[1+\frac{\mu}{\xi}K(\lambda_1^2)+2\lambda_1^2\frac{\mu}{\xi}K'(\lambda_1^2)\right]\right\}^{-1} \tag{42}$$

In the phantom network limit we may write

$$\frac{dv_2}{dr}=\frac{G}{r}[v_2(\lambda_2^2-\lambda_1^2)+2(\lambda_1^2 v_2-1)]\times\left[\frac{RT}{\bar{V}_1}\left(2\chi-\frac{1}{1-v_2}\right)v_2-G\lambda_1^2\right]^{-1} \tag{43}$$

Equation (43) is similar to the equation for radial change in volume fraction of polymer in a cylinder at equilibrium given by Treloar[17].

For a sphere, the analysis is identical except that the force balance expression is given by equation (20), and the extension ratios are given by equations (23) through (25), where subscripts 1, 2 and 3 correspond to r, θ and ϕ respectively. By substitution in a manner identical to that for the cylinder, the variation of polymer volume fraction with radial position is obtained.

$$\frac{dv_2}{dr}=\frac{2G}{r}\left\{v_2\left[\lambda_2^2-\lambda_1^2+\lambda_2^2\frac{\mu}{\xi}K(\lambda_2^2)-\lambda_1^2\frac{\mu}{\xi}K(\lambda_1^2)\right]+2v_2\lambda_1^2\left[1+\frac{\mu}{\xi}K(\lambda_1^2)+\lambda_1^2\frac{\mu}{\xi}K'(\lambda_1^2)\right]-\frac{2R}{r}\left[1+\frac{\mu}{\xi}K(\lambda_1^2)+\lambda_1^2\frac{\mu}{\xi}K'(\lambda_{21})\right]\right\}\times\left\{\frac{RT}{V_1}\left(2\chi-\frac{1}{1-v_2}\right)v_2-G\lambda_1^2\left[1+\frac{\mu}{\xi}K(\lambda_1^2)+2\lambda_1^2\frac{\mu}{\xi}K'(\lambda_1^2)\right]\right\}^{-1} \tag{44}$$

A complete specification of these equations is given by identifying $K(\lambda^2)$ and $K'(\lambda^2)$ according to equations (9) and (39). In the glassy core of the cylinder the θ and radial stresses are equal to each other and the radial stress at the outer radius of the glassy core. In the sphere, the ϕ stress is also equal to this radial stress[9].

MODEL PREDICTIONS

General observations

Solution of these expressions for a polymer system which exhibits Case-II behaviour gives the equilibrium polymer volume fraction in the sample. Knowledge of this volume fraction enables one to compute stresses in the swollen region as well as the total stress on the glassy core.

Equations (23) through (30) specify the required geometric constraints of the cylinder and sphere. Their solution for polymer volume fraction can be carried out by an iterative numerical procedure in which the quantity $v_2(r_c)$, where r_c is the radius of the glassy core, is assumed at the rubbery/glass interface, and equations (42) and (44) are used to compute $v_2(r)$. The solution must satisfy the boundary condition $\sigma_1(r_0)=0$, where r_0 is the outer radius of the sample. For the slab, dv_2/dr is zero everywhere and thus the solution of equation (36) is sufficient for complete specification of v_2.

A number of parameters can influence the equilibrium volume fraction behaviour in stressed as well as unstressed polymer systems. These include the penetrant–polymer interaction parameter, χ, the elastic modulus of the network, G, and the entanglement parameter, κ. Furthermore, in stressed systems which contain a glassy core, the radius of this core influences both stress and concentration profiles by establishing and controlling stress levels. Results describing the influence of these parameters are discussed below.

Systems of spherical and cylindrical geometry are characterized by certain distinct features. The polymer volume fraction is highest near the core and lowest at the outer boundary of the swollen rubbery shell. This

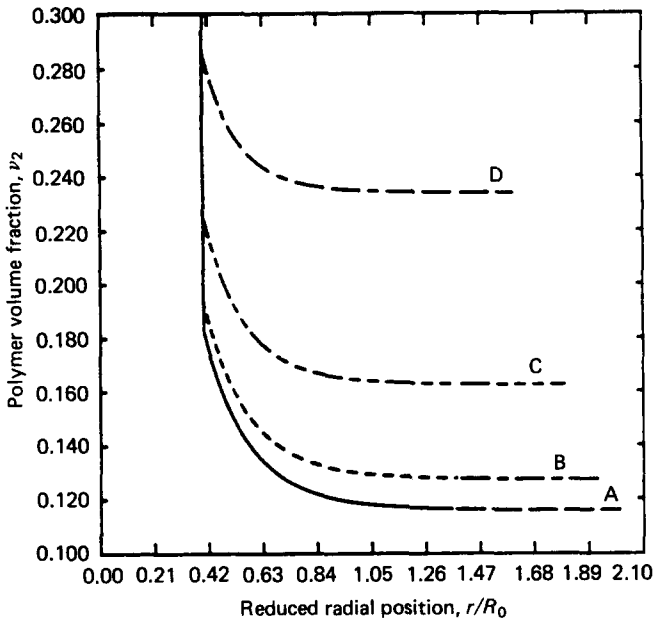

Figure 1 Polymer volume fraction, v_2, as a function of reduced radial position, r/R_0, for a spherical swelling polymer as a function of the penetrant–polymer interaction parameter χ. All curves are for initial modulus $G=0.4\,\mathrm{Nmm}^{-2}$ and entanglement parameter $\kappa=0$. Curve A with $\chi=-0.1$, curve B with $\chi=0.0$, curve C with $\chi=0.2$ and curve D with $\chi=0.4$

phenomenon arises from the non-homogeneous distribution of stresses in the system. A polymer element near the core experiences a larger deformation than one near the outer edge. Consequently the stress in this region is greater than in the outer regions. Since the stress influences the chemical potential, which in turn must be equal to that of the penetrant surrounding the sample and to that of the remainder of the swollen region, the concentration of the penetrant is decreased.

The stress profiles of these samples also exhibit the aforementioned behaviour. Radial stress is tensile and greatest near the core. Stresses in the θ and axial directions are compressive and are also greatest at the core of the sample. The stresses in the glassy core are computed from an equation that states that the net stress in the axial direction in the swollen region is supported by the glassy core. Consequently the axial stresses in the glassy portion are tensile. The radial and θ-stresses are identical[9] and are computed from the stress continuity condition at the glassy/rubbery interface.

Radial stresses approach the boundary condition, the value zero, at the outer boundary of the swollen rubbery portion. The θ-stresses and axial stresses are finite throughout the sample. The θ-stress arises due to the constraining nature of the glassy core and does not approach zero until the core vanishes. Likewise, the axial stress is a consequence of the constraining nature of the core in the axial direction and it abates only when the sample is fully relaxed following disappearance of the core.

Influence of the χ factor on stress and swelling

The penetrant–polymer interaction parameter, χ, in the Flory–Huggins analysis, defines the thermodynamic interaction between polymer and penetrant. A χ factor greater than zero represents an unfavourable enthalpy of interaction between polymer and penetrant, whereas one smaller than zero represents favourable interactions. Generally, mixing entropy changes may compensate for unfavourable enthalpic interactions.

The polymer volume fraction and radial stress profiles in a spherical polymer sample as a function of the factor χ are shown in *Figures 1* and *2*, respectively. As the χ factor increases from -0.1 to 0.4, the polymer volume fraction increases and the radial stress diminishes. This observation is consistent with the nature of χ as a polymer penetrant interaction parameter, since as interactions become more unfavourable the amount of penetrant decreases. The polymer volume fraction profile in a cylinder is qualitatively similar to that in the sphere as shown in *Figure 3*. The radial stress profile for the cylinder is shown in *Figure 4* and the axial-stress profile is shown in *Figure 5*. Note that the θ-stress in the glassy core region is equal to the radial stress. Finally, the θ-stress profile in the cylinder is shown in *Figure 6*. These stresses result from the constraint of the swollen rubbery annulus to its original unswollen axial dimension by the rigid glassy core. It must be noted that the stresses on the glassy core are tensile and those on the rubbery portion are compressive.

In general, higher degrees of swelling result in greater stresses due to the distortion of the network. Thus, more favourable polymer–penetrant interactions characterized by lower values of χ lead to greater degrees of swelling, balanced by larger stresses. The degree of swelling determines the outer radius of the swollen portion of the polymer sample.

Influence of modulus on stress and swelling

The influence of modulus, G, on polymer volume fraction and stress profile in swelling polymers for spherical geometries is shown in *Figures 7* and *8*. As the crosslinking density increases, G also increases.

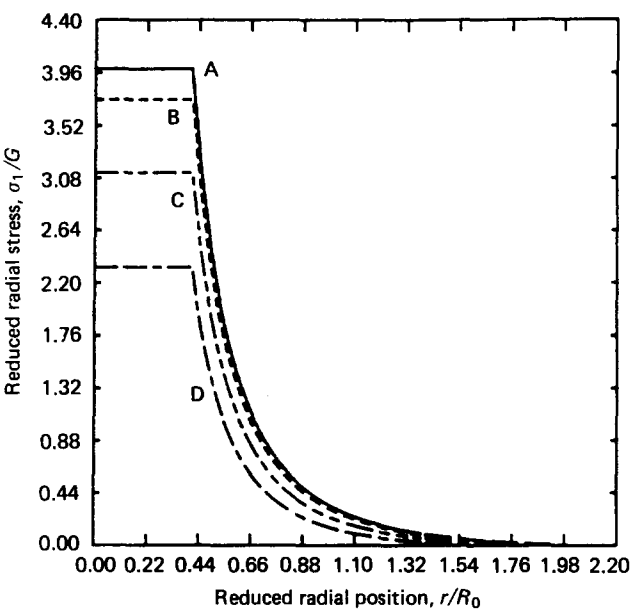

Figure 2 Reduced radial stress, σ_1/G, as a function of reduced radial position, r/R_0, for a spherical swelling polymer as a function of the penetrant–polymer interaction parameter χ. All curves are for initial modulus $G=0.4\,\mathrm{Nmm}^{-2}$ and entanglement parameter $\kappa=0$. Curve A with $\chi=-0.1$, curve B with $\chi=0.0$, curve C with $\chi=0.2$ and curve D with $\chi=0.4$

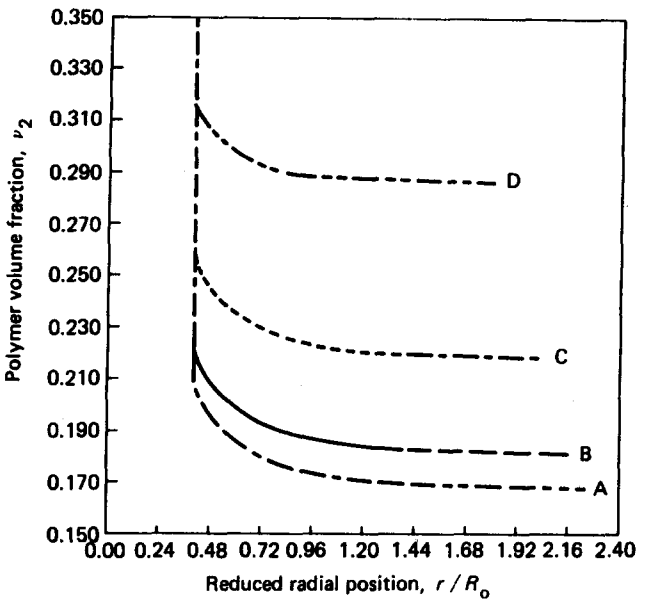

Figure 3 Polymer volume fraction, v_2, as a function of reduced radial position, r/R_0, for a cylindrical swelling polymer as a function of the penetrant–polymer interaction parameter χ. All curves are for initial modulus $G=0.4\,\mathrm{Nmm}^{-2}$ and entanglement parameter $\kappa=0$. Curve A with $\chi=-0.1$, curve B with $\chi=0.0$, curve C with $\chi=0.2$ and curve D with $\chi=0.4$

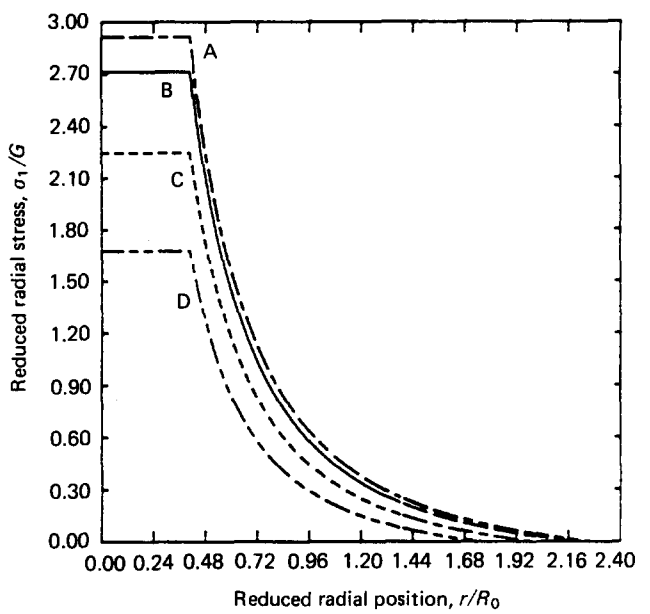

Figure 4 Reduced radial stress, σ_1/G, as a function of reduced radial position, r/R_0, for a cylindrical swelling polymer as a function of the penetrant–polymer interaction parameter χ. All curves are for initial modulus $G=0.4\,\mathrm{Nmm}^{-2}$ and entanglement parameter $\kappa=0$. Curve A with $\chi=-0.1$, curve B with $\chi=0.0$, curve C with $\chi=0.2$ and curve D with $\chi=0.4$

Figure 7 shows the influence of modulus on the equilibrium polymer volume fraction in spheres. The modulus of the network directly affects the degree of swelling. A highly crosslinked system exhibits greater resistance to any deformation including deformations associated with swelling. Thus, as crosslinks are incorporated into a network the degree of swelling decreases and polymer volume fraction rises.

Both the degree of swelling of a polymer element and the stress exhibited as a result of a given deformation are related to the modulus and consequently to the degree of crosslinking of the sample. *Figure 8* demonstrates the effect of a very high modulus on radial stress in a spherical sample. Initially the stresses rise with increasing modulus despite simultaneous reduction in the degree of swelling of the sample. Eventually, at sufficiently large modulus,

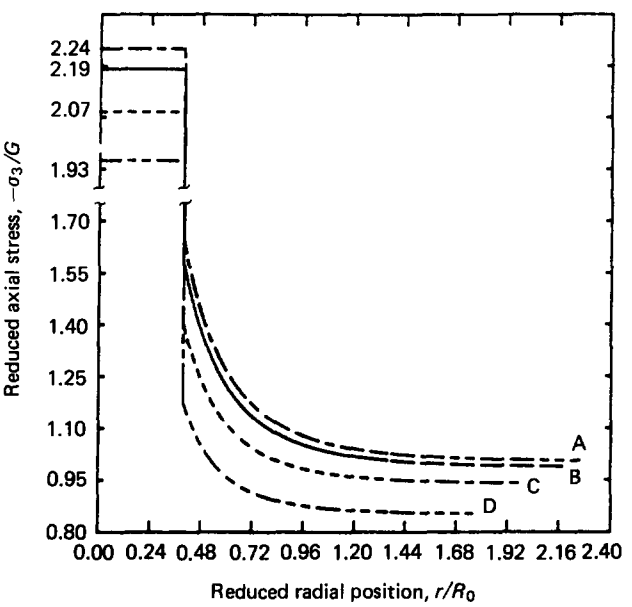

Figure 5 Absolute reduced axial stress, $-\sigma_3/G$, as a function of reduced radial position, r/R_0, for a cylindrical swelling polymer as a function of the penetrant–polymer interaction parameter χ. All curves are for initial modulus $G=0.4\,\mathrm{Nmm}^{-2}$ and entanglement parameter $\kappa=0$. Curve A with $\chi=-0.1$, curve B with $\chi=0.0$, curve C with $\chi=0.2$ and curve D with $\chi=0.4$

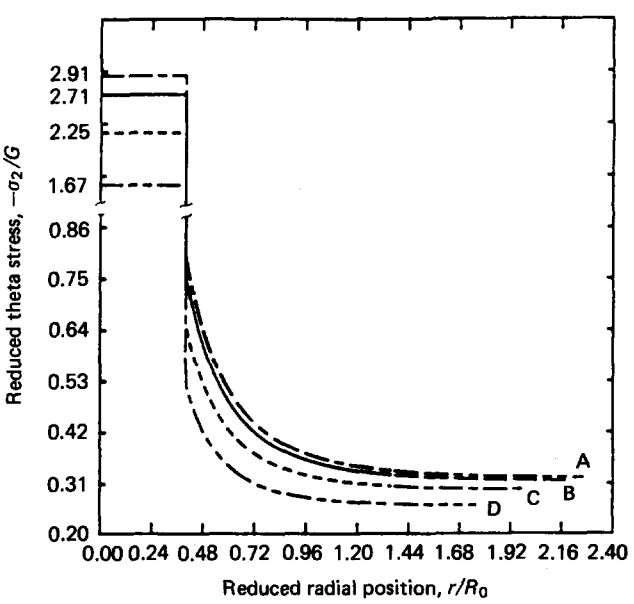

Figure 6 Absolute reduced θ-stress, $-\sigma_2/G$, as a function of reduced radial position, r/R_0, for a cylindrical swelling polymer as a function of the penetrant–polymer interaction parameter χ. All curves are for initial modulus $G=0.4\,\mathrm{Nmm}^{-2}$ and entanglement parameter $\kappa=0$. Curve A with $\chi=-0.1$, curve B with $\chi=0.0$, curve C with $\chi=0.2$ and curve D with $\chi=0.4$

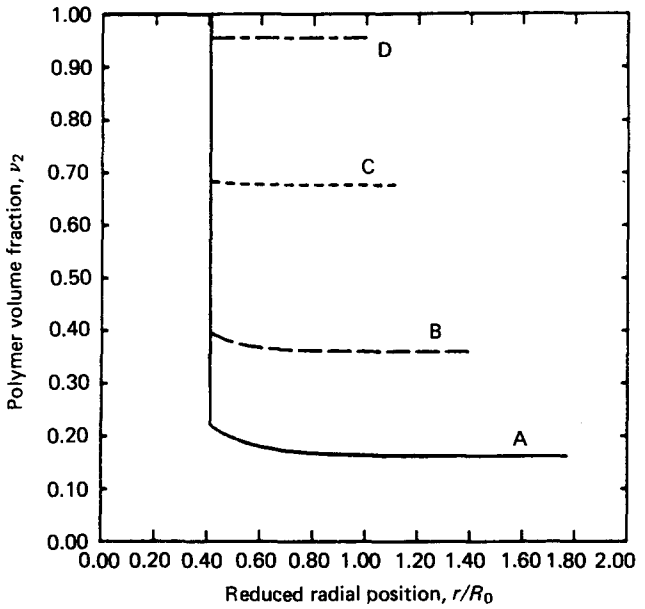

Figure 7 Polymer volume fraction, v_2, as a function of reduced radial position, r/R_0, for a spherical swelling polymer as a function of the modulus G (Nmm^{-2}). All curves are for the penetrant–polymer interaction parameter $\chi = 0.2$ and entanglement parameter $\kappa = 0$. Curve A with $G = 0.4$, curve B with $G = 2.0$, curve C with $G = 10.0$ and curve D with $G = 50.0$

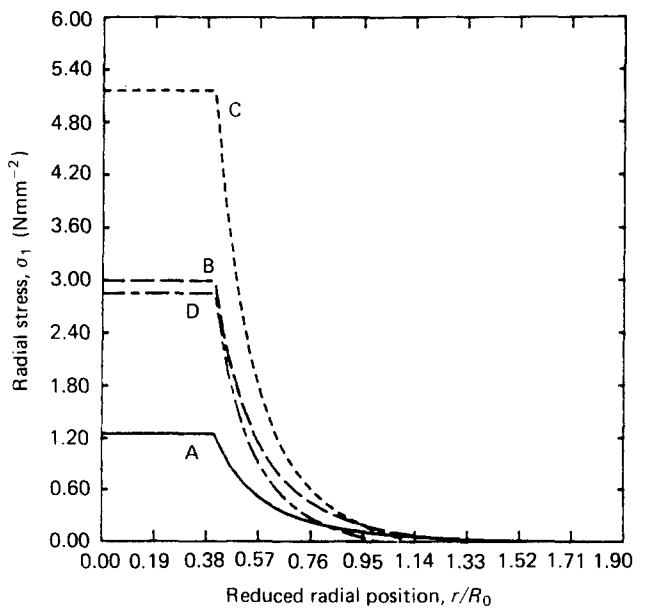

Figure 8 Absolute radial stress, σ_1 (Nmm^{-2}), as a function of reduced radial position, r/R_0, for a spherical swelling polymer as a function of the modulus G (Nmm^{-2}). All curves are for the penetrant–polymer interaction parameter $\chi = 0.2$ and entanglement parameter $\kappa = 0$. Curve A with $G = 0.4$, curve B with $G = 2.0$, curve C with $G = 10.0$ and curve D with $G = 50.0$

the degree of swelling and associated distortions become very small. This phenomenon leads to a drop in the network stresses.

Influence of entanglements on stress and swelling

The entanglement parameter, κ, governs the junction fluctuations about the centres of their domains of constraint. A value of κ near zero gives rise to the familiar phantom network model of rubber elasticity and a very large value of κ corresponds to a highly entangled system which is described by the affine model of Flory[13]. The parameter κ increases with increasing network entanglements.

The influence of κ on the volume fraction in the sphere is seen in *Figure 9*. Since κ represents the degree of entanglement of the polymer network, a non-zero value of κ reflects additional restrictions on the network above the phantom limit. Networks which exhibit appreciable degrees of entanglement tend to swell less than those without entanglements due to their contribution to the network elasticity. The influence of κ on the radial stress in the sphere is shown in *Figure 10*. The net decrease in swelling with increasing κ gives rise to lower values of swelling induced stress.

Effect of glassy core radius on stress and swelling

The radius of the glassy portion of the polymer influences both the stress and volume fraction profiles in cylindrical and spherical samples. Large values of the radius of the glassy portion normalized with respect to the radius of the glassy portion prior to swelling, r_c/R_0, give higher distortions of the polymer in the adjacent rubbery region. Since homogeneous swelling corresponds to zero deformation, the closer the system is to a homogeneously swollen one, the less distorted the outer rubbery portion will be. Thus, samples with large glassy cores exhibit larger polymer volume fractions in the rubbery portion than those with small cores or no core at all.

The polymer volume fraction profiles for a spherical polymer are presented in *Figure 11*. As the core decreases, the polymer volume fraction approaches the independently obtained values of 0.15 for the homogeneously swollen sphere and 0.20 for the coreless but still constrained cylinder. Both of these systems have χ-factors of 0.2 and G values of 0.4 Nmm^{-2}. *Figure 12*

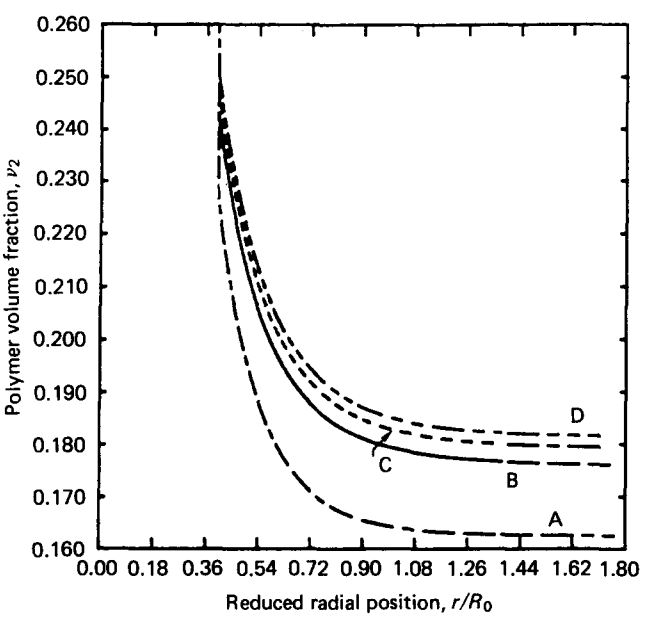

Figure 9 Polymer volume fraction, v_2, as a function of reduced radial position, r/R_0, for a spherical swelling polymer as a function of the junction entanglement parameter κ. All curves are for initial modulus $G = 0.4$ Nmm^{-2} and penetrant–polymer interaction parameter $\chi = 0.2$. Curve A with $\kappa = 0.0$, curve B with $\kappa = 8.0$, curve C with $\kappa = 24.0$ and curve D with $\kappa = 200.0$

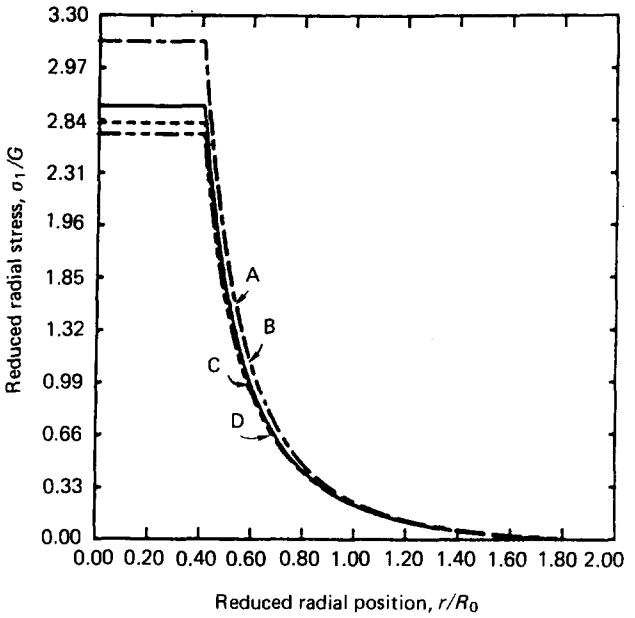

Figure 10 Absolute reduced radial stress, σ_1/G, as a function of reduced radial position, r/R_0, for a spherical swelling polymer as a function of the junction entanglement parameter κ. All curves are for initial modulus $G=0.4\,\mathrm{Nmm^{-2}}$ and penetrant–polymer interaction parameter $\chi=0.2$. Curve A with $\kappa=0.0$, curve B with $\kappa=8.0$, curve C with $\kappa=24.0$ and curve D with $\kappa=200.0$

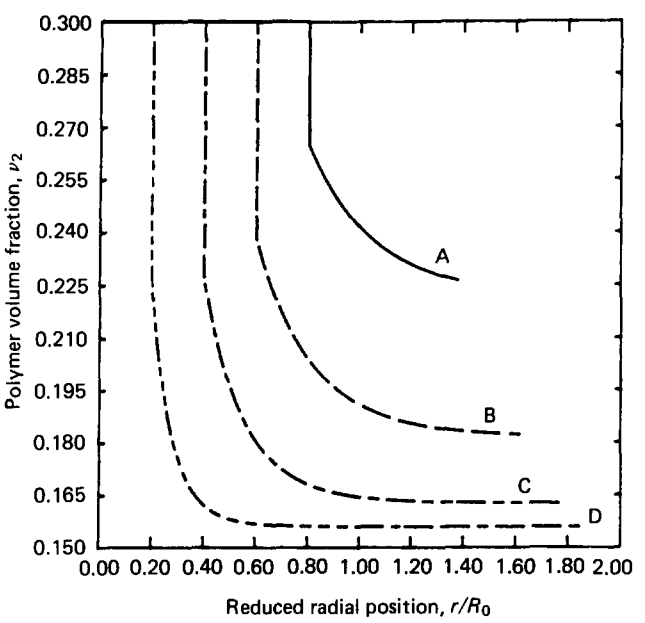

Figure 11 Polymer volume fraction, ν_2, as a function of reduced radial position, r/R_0, for a spherical swelling polymer as a function of the reduced glassy core radius r_c/R_0. All curves are for initial modulus $G=0.4\,\mathrm{Nmm^{-2}}$, entanglement parameter $\kappa=0$ and penetrant–polymer interaction parameter $\chi=0.2$. Curve A with $r_c/R_0=0.8$, curve B with $r_c/R_0=0.6$, curve C with $r_c/R_0=0.4$ and curve D with $r_c/R_0=0.2$

shows the profiles of stresses for spheres with glassy cores of differing diameters.

The radial stress increases somewhat at the core but falls to lower asymptotic values with decreasing core diameter. For the cylinder, the axial stress approaches a plateau value which results from the constraint of the glassy core in the axial direction. Since this axial stress is supported by the glassy core and the glassy core diminishes to a zero radius, there must exist a point at which the stresses supported by the core overcome the strength of the core. In this case the core either breaks or undergoes sudden elongation. The relief of stresses upon breakup or elongation of the core can lead to an increase in the equilibrium penetrant volume fraction for the polymer sample. This increase may lead to Super Case-II or two stage sorption, since, once the core has broken, the sample can resume sorption to its new higher equilibrium penetrant volume fraction. This anomalous sorption has been described by Windle[1] and can be explained by stress release upon core breakup. According to the present framework, similar effects would not be seen in spheres.

Stress and swelling behaviour in discs and slabs

The stress and equilibrium swelling of discs and slabs undergoing Case-II transport is considerably simpler than that for cylinders and spheres. The polymer volume fraction is given by equation (36). The stresses and volume fractions do not change throughout the rubbery portion. However, y- and z-stresses per area of the glassy portion increase rapidly as the glassy portion diminishes in size since the glassy portion supports the rubbery portion. The values of stress and polymer volume fraction for different values of χ and modulus are given in *Table 1*. The violent breakup of swelling polymer discs observed by Alfrey *et al.*[9] represents a dramatic manifestation of the stress build-up in swelling of slabs and discs.

CONCLUSIONS

An analysis has been presented which may be used in conjunction with the relationships between stresses and equilibrium swelling to compute equilibrium volume

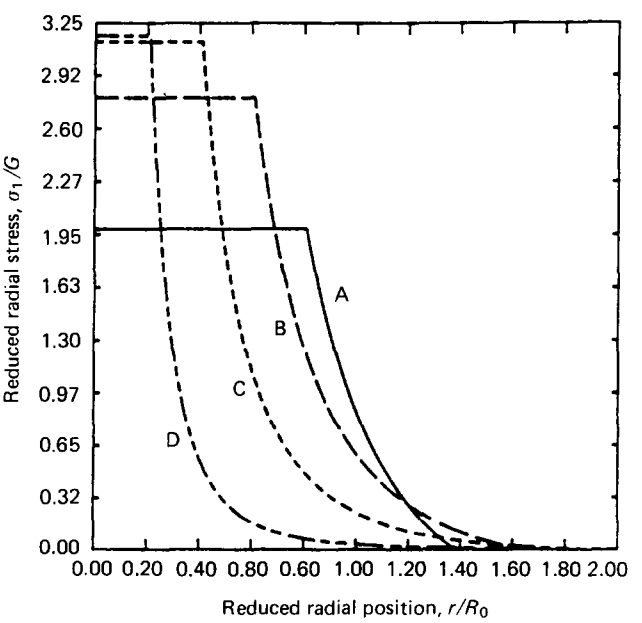

Figure 12 Absolute reduced radial stress, σ_1/G, as a function of reduced radial position, r/R_0, for a spherical swelling polymer as a function of the reduced glassy core radius r_c/R_0. All curves are for initial modulus $G=0.4\,\mathrm{Nmm^{-2}}$, entanglement parameter $\kappa=0$ and penetrant–polymer interaction parameter $\chi=0.2$. Curve A with $r_c/R_0=0.8$, curve B with $r_c/R_0=0.6$, curve C with $r_c/R_0=0.4$ and curve D with $r_c/R_0=0.2$

Table 1 Stress and polymer volume fraction in slabs and discs

Modulus G ($N\,mm^{-2}$)	Interaction parameter (χ)	Stress $-\sigma_3$ ($N\,mm^{-2}$)	Polymer volume fraction (v_2)
0.2	0.2	0.689	0.269
0.8	0.2	1.668	0.334
3.2	0.2	3.660	0.580
24.0	0.2	6.098	0.881
200.0	0.2	0.400	0.999
0.4	−1.0	1.311	0.281
0.4	0.0	1.243	0.294
0.4	0.2	1.084	0.329
0.4	0.4	0.888	0.384

fractions and stress profiles in systems which exhibit Case-II transport. The analysis employs a recent statistical thermodynamic model for rubber elasticity developed by Flory and Erman[13], which considers the constraints on junction fluctuations by network entanglements. It has been previously demonstrated that this model shows good agreement with experimental data surpassing simpler models[14].

Analysis of equilibrium stress and Case-II swelling reveals behaviour previously not considered in theoretical treatments of this problem. Principally, the changes in equilibrium concentration with radius and changes in average equilibrium concentration with changing glassy core diameter in spheres and cylinders are consequences of the non-homogeneous stress distribution in samples with glassy cores. This distribution can greatly influence the diffusion coefficient of a solute being released from a network, due to the exponential dependence of the solute diffusion coefficient on penetrant concentration[18]. Furthermore, breakup of the core in cylindrical and planar samples leads to an increase in equilibrium concentration of penetrant due to relief of constraining stresses. This increase may be associated with the anomalous or super Case-II acceleration of sorption rates discussed by Windle[1]. It is therefore possible to compute all of the stresses leading to the breakup of a glassy core.

The swelling and stress–strain behaviour of an elastic network is controlled by certain molecular parameters: the χ factor, degree of entanglement, and degree of crosslinking. In addition, physical constraints on the system such as the presence of a glassy core can significantly influence the swelling behaviour of a rubbery system. The preceding discussion has provided examples of the influence of all of these factors on the stress and swelling behaviour of polymers undergoing Case-II transport.

ACKNOWLEDGEMENTS

This work was supported in part by NSF grants INT-84-12692 and CPE-82-07381.

REFERENCES

1 Windle, A. H. in 'Polymer Permeability' (Ed. J. Comyn), Elsevier, London, 1985, p. 108
2 Frisch, H. L., Wang, T. T. and Kwei, T. K. *J. Polym. Sci., A-2* 1969, **7**, 879
3 Peterlin, A. *J. Polym. Sci.* 1965, **B3**, 1083
4 Peterlin, A. *Makromol. Chem.* 1969, **124**, 136
5 Joshi, S. and Astarita, G. *Polymer* 1979, **20**, 455
6 Astarita, G. and Nicolais, L. *Pure Appl. Chem.* 1983, **55**, 727
7 Thomas, N. L. and Windle, A. H. *Polymer* 1982, **23**, 520
8 Durning, C. J. *J. Polym. Sci., Polym. Phys. Edn* 1985, **23**, 1831
9 Alfrey, T., Gurnee, E. F. and Lloyd, W. G. *J. Polym. Sci.* 1969, **C12**, 249
10 Valanis, K. C. and Landel, R. F. *J. Appl. Phys.* 1969, **38**, 2997
11 Treloar, L. R. G. 'The Physics of Rubber Elasticity', Oxford University Press, Oxford, 1975
12 Flory, P. J. *J. Chem. Phys.* 1977, **66**, 5720
13 Flory, P. J. and Erman, B. *Macromolecules* 1982, **15**, 800
14 Erman, B. and Flory, P. J. *Macromolecules* 1982, **15**, 806
15 Erman, B. *J. Polym. Sci., Polym. Phys. Edn* 1983, **21**, 893
16 Williams, J. G. 'Stress Analysis in Polymers', Wiley, New York, 1973
17 Treloar, L. R. G. *Polymer* 1976, **17**, 142
18 Korsmeyer, R. W., Lustig, S. R. and Peppas, N. A. *J. Polym. Sci., Polym. Phys. Edn* 1986, **24**, 395